Biochemistry

 Volume 30, Number 39 October 1, 1991

Articles

^{1}H NMR and Circular Dichroism Studies of the N-Terminal Domain of Cyclic GMP Dependent Protein Kinase: A Leucine/Isoleucine Zipper

R. Andrew Atkinson, Vladimir Saudek, John P. Huggins, and John T. Pelton*
Marion Merrell Dow Research Institute, 16 rue d'Ankara, BP 447/R9, 67009 Strasbourg Cedex, France
Received March 11, 1991; Revised Manuscript Received June 17, 1991

ABSTRACT: Cyclic GMP dependent protein kinase exists as a dimer in its native form. A peptide corresponding to the dimerization domain in the N-terminal segment has been characterized by circular dichroism, ultracentrifugation, and ^{1}H NMR spectroscopy. The peptide (G-kinase$_{1-39}$ amide) is shown to be dimeric in solution. Determination of the molecular weight of the species in solution from the sedimentation coefficient and diffusion coefficient yields a value more than twice that of the monomeric species. Circular dichroism studies show G-kinase$_{1-39}$ amide to be largely helical in aqueous solution and stable over a wide range of pH and temperature. The conformational stability is found to be concentration dependent, the peptide having a melting temperature of 75 °C (at 20 μM and pH 4.0). The assignment of the ^{1}H NMR spectrum and analysis of the patterns of nuclear Overhauser enhancements confirm the helical nature of the conformation. Distance geometry calculations result in a well-defined helical structure containing a kink near Ser 26. The dimerization of G-kinase is most likely to occur through the hydrophobic interaction of leucine and isoleucine side chains located on one face of a helical structure with supporting electrostatic interactions between flanking side chains. The dimerization domain of G-kinase is clearly analogous to the "leucine zipper" motifs found in a number of DNA transcriptional activators.

Cyclic GMP dependent protein kinase (G-kinase)[1,2] is an enzyme composed of 670 amino acids (M_r 76 000), the native form of which was identified as a dimer of molecular weight ca. 155 000 (Gill et al., 1977; Lincoln et al., 1977). G-Kinase has been identified as a major receptor protein for cGMP [for review, see Edelman et al. (1987)], and although levels of G-kinase are low compared to levels of cyclic AMP dependent protein kinase (A-kinase) in most tissues, it is found in appreciable concentrations in the cerebellum (Hofmann & Sold, 1972; Lohmann et al., 1981), smooth muscle (Kuo, 1974; Ecker et al., 1989), and lung (Gill et al., 1976). In smooth muscle, the enzyme has been implicated in mediating the relaxation induced by agents which elevate cGMP concentrations (Fiscus et al., 1984).

Four functional domains have been identified in the primary sequence of G-kinase (Takio et al., 1984). The N-terminal domain (comprising the first 100 residues) has been shown to contain the portion of the sequence responsible for dimerization, a hinge region, and the major autophosphorylation site at Thr 58 (Monken & Gill, 1980; Takio et al., 1983, 1984; Aitken et al., 1984). Two cGMP-binding domains follow in the sequence, and these show high homology with the cAMP-binding domains of A-kinase. The fourth domain contains the substrate binding sites.

The N-terminal domain has been shown to be involved in the regulation of enzyme activity by investigating the effects of (i) autophosphorylation on cyclic nucleotide binding

* Author to whom correspondence should be addressed.

[1] Abbreviations: G-kinase$_{1-39}$ amide, residues 1–39 of the Iα isoform of G-kinase with a C-terminal amide group; G-kinase, cyclic GMP dependent protein kinase; A-kinase, cyclic AMP dependent protein kinase; cGMP, cyclic GMP; cAMP, cyclic AMP; CD, circular dichroism; rpm, revolutions per minute; NMR, nuclear magnetic resonance spectroscopy; NOE, nuclear Overhauser enhancement; COSY, 2-D correlated spectroscopy; TOCSY, 2-D totally correlated spectroscopy; NOESY, 2-D nuclear Overhauser enhancement spectroscopy; ppm, parts per million; rmsd, root mean square distance. Standard one-letter codes and three-letter abbreviations for the amino acids are used throughout. Interproton NOEs are denoted by the shorthand dAB$_{i+n}$, where A and B refer to the two protons and n is an integer indicating the separation of the two residues in the sequence (thus dNN$_{i+1}$ denotes an NOE between the NH resonances of adjacent residues). In Figure 7, $(\Delta\delta_\alpha)_{\pm 2}$ refers to the mean secondary chemical shift calculated by using a smoothing window of ±2 residues.

[2] This paper refers to the Iα isoform of G-kinase unless otherwise stated.

0006-2960/91/0430-9387$02.50/0

(Hofmann et al., 1985; Landgraf et al., 1986), (ii) chemical modification of arginine residues in the N-terminal domain (Lincoln et al., 1978), and (iii) proteolytic removal of the N-terminal segment (Heil et al., 1987; Landgraf & Hofmann, 1989). The autophosphorylation site in the N-terminal segment is thought to be responsible for autoinhibition of G-kinase in the absence of cGMP [see Soderling (1990)]. It is not clear, however, whether autoinhibition of the catalytic site of one subunit of the dimer is effected by the N-terminal segment of the same subunit or that of the opposite subunit. While proteolytic activation resulted in a monomeric species (Heil et al., 1987), this proteolysis removed both the dimerization and autophosphorylation sites. Furthermore, a form of the Iβ isoform of G-kinase can be produced by proteolysis, which is monomeric but still requires cGMP for activation (Wolfe et al., 1989). In either case, binding of cGMP might then induce a conformational change involving the N-terminal segment which results in catalysis.

Secondary structure prediction by Chou–Fasman analysis (Chou & Fasman, 1977) of the N-terminal region of bovine G-kinase indicated that the first 38 residues should adopt, almost exclusively, an α-helical conformation (Landgraf et al., 1990). Furthermore, a leucine or isoleucine residue was noted at every seventh position between residues 11 and 53, reminiscent of the "leucine zipper" motif identified in a number of DNA transcriptional activators [e.g., Landschulz et al. (1988) and Kouzarides and Ziff (1989)]. In the leucine zipper motif, a leucine side chain at every seventh position in a helical structure creates a hydrophobic stripe on one face of the helix which allows dimerization with another such helix [see Landschulz et al. (1988)]. In DNA transcriptional activators (e.g., GCN4, jun, fos) the leucine zipper domains serve to dimerize and to position the preceding basic domains to enable binding to DNA. The identification of a heptad repeat alone is not a guarantee of the presence of a leucine zipper structure (Brendel & Karlin, 1989), but circular dichroism (CD) studies of a synthetic peptide corresponding to the N-terminal 39 residues of bovine G-kinase (G-kinase$_{1-39}$ amide) indicated a predominantly α-helical structure in solution (Landgraf et al., 1990). In addition, the sequence of a second isoform of G-kinase (Iβ) found in aortic and tracheal smooth muscle (Lincoln et al., 1988; Wernet et al., 1989; Wolfe et al., 1989), which differs from the sequence of the Iα isoform in the N-terminal region, was also found to contain the heptad repeat of leucine or isoleucine residues (Landgraf et al., 1990).

In this paper, we report further detailed biophysical studies of the N-terminal region of G-kinase (Iα). Circular dichroism studies have been extended to assess the degree of helical character and the stability of the structure to variation in temperature and pH. The molecular weight in solution has been estimated by ultracentrifugation in order to establish whether G-kinase$_{1-39}$ amide exists in solution as a monomer, dimer, or higher oligomer. Nuclear magnetic resonance (NMR) experiments have been performed to define the conformation of the peptide in solution more precisely. The structure of the monomer has been calculated by distance geometry methods. The implications of the results are discussed with reference both to the dimerization of G-kinase and to the comparison of the N-terminal sequence with the leucine zipper motif, which serves to dimerize a number of DNA transcriptional activators.

Experimental Procedures

Peptide Synthesis. G-Kinase$_{1-39}$ amide was synthesized, purified, and analyzed as described previously (Landgraf et al., 1990).

Circular Dichroism. Circular dichroism spectra were measured with an Aviv Model 62DS spectropolarimeter and water-jacketed, dichroically neutral quartz cuvettes. The same solvent was used as for the NMR experiments, i.e., ^1H_2O containing 10% ^2H_2O. All pH values are direct meter readings uncorrected for isotope effect. For all measurements, a 1.5-nm bandwidth and a 3.0-s time constant were used. Three scans were averaged for each spectrum, which was then corrected for solvent contributions and fitted by nonlinear regression analysis. Measured rotations were converted to mean residual ellipticity prior to analysis.

(*i*) *pH Studies.* Spectra were measured between 300 and 185 nm at 40 °C with solutions of G-kinase$_{1-39}$ amide at 20 μM and pH values in the range 2.1–10.1. The pH of the solutions was adjusted with small aliquots of solutions of NaOD and DCl in ^2H_2O. A cuvette with a path length of 2.0 mm was used, and the step size was set to 0.5 nm.

(*ii*) *Temperature Studies.* A set of spectra were measured between 300 and 185 nm with a solution of G-kinase$_{1-39}$ amide at 17 μM and pH 4.0, at temperatures in the range 5–80 °C. A cuvette with a path length of 1.0 mm was used, and the step size was set to 0.5 nm.

A further set of temperature studies were performed at differing concentrations. Solutions of G-kinase$_{1-39}$ amide were prepared at concentrations of 2, 20, and 200 μM, and spectra were recorded by using cuvettes with path lengths of 1.00, 0.10, and 0.01 cm, respectively. Spectra were measured in the range 5–93 °C as described above but only between 270 and 200 nm and with a step size of 2 nm. Data were corrected for inaccuracies in path length or concentration by using the absorbance at 210 nm, derived from the dynode voltage recorded at the same time as the CD spectrum.

(*iii*) *Secondary Structure Estimates.* The estimated percentage of α-helical structure was calculated from the CD spectra with the program PROSEC (PROtein SECondary structure estimator v2.1, Aviv Associates, Lakewood, NJ), based upon the method of Chang et al. (1978). The quality of the estimates was assessed by recalculating the CD spectra with the program BLEND (Aviv Associates, Lakewood, NJ).

Molecular Weight Determination by Ultracentrifugation. The molecular weight of G-kinase$_{1-39}$ amide in solution was measured by determination of the sedimentation coefficient and diffusion coefficient (Schachman, 1957; Chervenka, 1969). A solution containing 0.15 mM peptide in 0.15 M sodium chloride was used. The sedimentation coefficient, s (in seconds), was calculated by measuring the displacement of the schlieren peak with time, at a rotor speed of 50 000 rpm. The diffusion coefficient, D (in cm^2 s^{-1}), was calculated from the broadening of the schlieren peak with time, at a rotor speed of 5000 rpm.

The molecular weight of G-kinase$_{1-39}$ amide, M_r, was calculated from the sedimentation coefficient and diffusion coefficient:

$$M_r = \left(\frac{RT}{1 - \nu\rho}\right)\frac{s}{D} \qquad (1)$$

where R is the gas constant, T is temperature (K), ν is the partial molar volume of the peptide (cm^3 g^{-1}), and ρ is the density of the solution (g cm^{-3}). Measurements were made at 296 K. The partial molar volume, ν, for G-kinase$_{1-39}$ amide was estimated (Cohn & Edsall, 1943) to be 0.756 cm^3 g^{-1} from the known amino acid composition (see Figure 1). The density of the solution, ρ, was taken to be that of 0.15 M sodium chloride at 20 °C (1.006 g cm^{-3}).

Nuclear Magnetic Resonance Experiments. All NMR experiments (except the NH exchange studies; see below) were performed with samples containing 3.3 mM peptide in ^2H_2O or ^1H_2O containing 10% ^2H_2O. The samples were adjusted to pH 4.0 (meter reading uncorrected for isotope effect) with small aliquots of solutions of NaOD and DCl in ^2H_2O. Sodium 3-(trimethylsilyl)propionate-d_4 was used as an internal reference set at 0.00 ppm.

All spectra used for the assignment and structural analysis of the peptide were recorded at 50 °C and 500 MHz on a Bruker AM500 spectrometer, equipped with an Aspect 3000 computer and a digital phase shifter. All 2-D experiments [COSY (Aue et al., 1976; Marion & Wüthrich, 1983), TOCSY (Braunschweiler & Ernst, 1983; Bax & Davis, 1985; Rance, 1987), and NOESY (Jeener et al., 1979; Anil-Kumar et al., 1980)] were acquired in the phase-sensitive mode using time-proportional phase incrementation (Marion & Wüthrich, 1983) with the transmitter set on the ^1H_2O resonance and using CYCLOPS phase cycling (Hoult & Richards, 1975).

NOESY spectra were recorded with mixing times of 150 and 200 ms and with a 10% random variation of the mixing time to eliminate zero-quantum transfer (Macura et al., 1981). TOCSY experiments used a radio-frequency field strength of 5–7 kHz and mixing times of 33, 50, and 67 ms. Solvent suppression was achieved by irradiation of the ^1H_2O resonance during the relaxation time (1.5 s) and during the mixing time of NOESY experiments.

Typically, 512 t_1 increments were acquired for each experiment with 16 transients and 2 dummy transients per increment. In t_2, 2048 data points were acquired over a spectral width of 5 or 4.25 kHz (for spectra recorded in ^2H_2O). All spectra were processed offline on a Bruker X32 workstation with the manufacturer's program UXNMR. Prior to Fourier transformation in t_2, the free induction decays were multiplied by a Gaussian function (for NOESY and TOCSY experiments) or an unshifted sine-bell function (for COSY experiments). The data were multiplied by a cosine bell (for NOESY and TOCSY experiments) or a sine bell (for COSY experiments) in t_1 and zero-filled to 2048 data points before the second Fourier transformation. The baseline was fitted with a third-order polynomial in both directions and subtracted from the spectra. The spectra are shown unsymmetrized with the *F*2 dimension horizontal and the contour levels spaced logarithmically.

(*i*) *Chemical Shift Analysis.* The deviations of the chemical shifts of the $C^\alpha H$ resonances from "random coil" values were analyzed according to the methods described by Pastore and Saudek (1990). A smoothing window of ±2 residues was used to removed local effects.

(*ii*) *Analysis of NOEs.* The intensity of observed NOEs was recorded as strong, medium, or weak, according to the appearance of the cross-peak in the NOESY spectra.

(*iii*) *Measurement of NH Exchange.* To detect backbone amide (NH) protons which exchange slowly into ^2H_2O, a sample of G-kinase$_{1-39}$ amide in ^1H_2O (containing 10% ^2H_2O) was lyophilized and redissolved in 500 μL of 10% acetic acid-d_4 in ^2H_2O. A NOESY experiment was recorded as described above but at pH 3.2 and 310 K, and those NH protons whose resonances were observed were classified as slowly exchanging.

Distance Geometry Calculations. Distance constraints were derived from NOESY spectra recorded with mixing times of 200 ms. Due to possible contributions to NOE intensity arising from intermonomer spatial proximities, accurate distance calibration was not attempted. Cross-peak intensity was classified as strong, medium, or weak according to the appearance of the cross-peak in the spectrum and assigned a distance of 0.3, 0.4, or 0.5 nm, respectively. Pseudoatom corrections were added to interproton distances where necessary (Wüthrich et al., 1983).

Over 7000 structures were calculated with the distance geometry program DISMAN (Braun & Go, 1985), using the list of distances as upper limit constraints and the sum of van der Waals radii as lower limit constraints between nonbonded atoms. Initial structures were generated from both random sets of dihedral angles and sets corresponding to helical backbone conformations. Pairwise rmsd values were calculated within the SYBYL molecular modeling package (Tripos Associates, St. Louis, MO, version 5.4).

Results and Discussion

Sequence Analysis. The N-terminal 70 residues of G-kinase have been identified as containing the region responsible for dimerization (Takio et al., 1984). The suggestion that the sequence of the N-terminal region resembles the leucine zipper motif, identified and characterized in a number of DNA transcriptional activators (Landschulz et al., 1988; Kouzarides & Ziff, 1989; White & Weber, 1989; Saudek et al., 1990), is reinforced by comparison with the sequence of the second isoform of G-kinase. The two isoforms of G-kinase, Iα and Iβ, have closely homologous amino acid sequences which differ, however, in the N-terminal region (Sandberg et al., 1989; Wernet et al., 1989). Although there is considerable dissimilarity between the Iα and Iβ N-terminal sequences, both share the heptad repeat motif. The limited homology in this region allows alignment of the sequences as shown in Figure 1a. The alignment presented here differs from that suggested previously (Landgraf et al., 1990) by a shift of seven residues of one sequence relative to the other, giving a greater degree of conservation of leucine and isoleucine residues and of residues with side chains carrying charged groups and also bringing the proline residue in each sequence (at position 47 in the Iα isoform) closer together.

The arrangement of the sequence in an α-helical structure may be modeled schematically as shown in Figure 1b,c. The "helical wheel" representation (Figure 1b) shows the hydrophobic side chains to be clustered on one side of such a structure, where residues are largely conserved between the two isoforms. The disposition of the residues along the helix is shown more clearly in Figure 1c. The alternating leucine and isoleucine side chains at every seventh position in the sequence form a conserved hydrophobic stripe on the surface of the α-helix, which is bordered by a stripe of negative charge (also conserved between the two isoforms) on one side and a conserved positive–hydrophobic stripe (K-L-K-L) on the other side. Note that for clarity the helical wheel representation (Figure 1b) is shown as a helix with a pitch of 3.5 residues/turn (as found in coiled-coil structures). A pitch of 3.6 residues/turn in an α-helix causes the stripes to curve around the surface of the model as shown in Figure 1c.

Analysis of the sequence therefore suggests that the dimerization of G-kinase might be achieved through a "leucine/isoleucine zipper" in which the hydrophobic interaction between the leucine/isoleucine stripes is complemented by the interaction of the oppositely charged stripes on either side. The following biophysical studies sought to further define the structural characteristics of G-kinase$_{1-39}$ amide in solution, in order to determine the nature of the N-terminal domain of G-kinase and to assess its relation to the leucine zipper motif.

Circular Dichroism Studies. From previous CD studies, G-kinase$_{1-39}$ amide is known to be largely α-helical in structure at pH 7.0 and 30 °C (Landgraf et al., 1990). Further CD

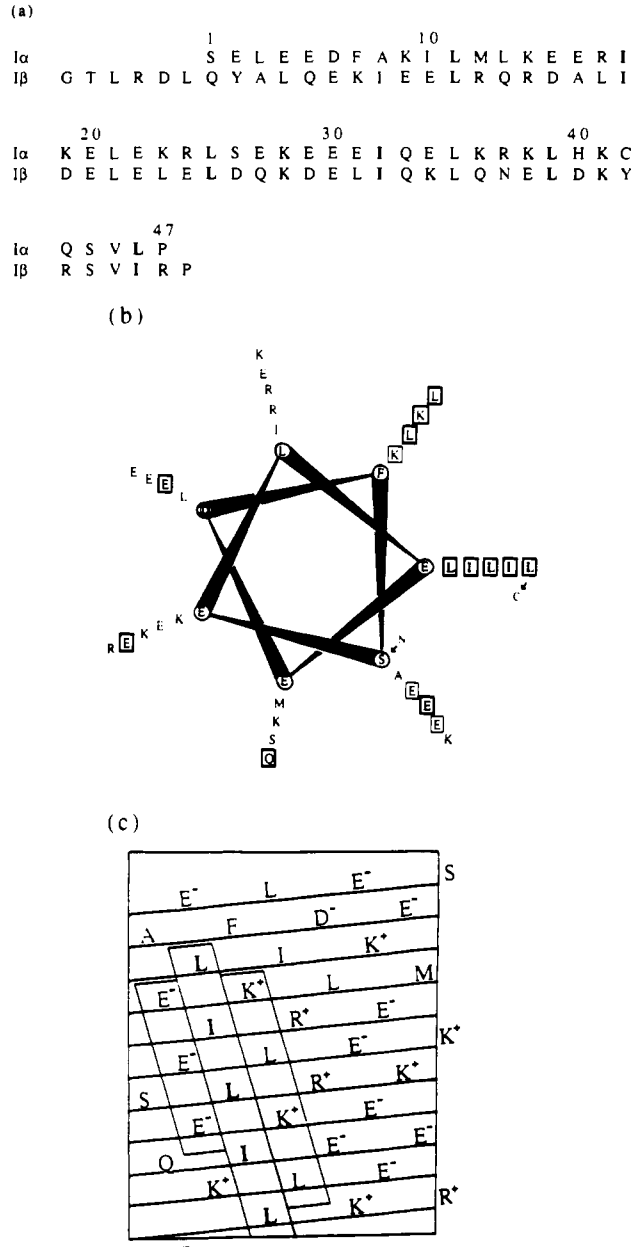

FIGURE 1: Analysis of the amino acid sequence of the N-terminal segment of G-kinase. The heptad repeat of leucine and isoleucine residues is highlighted in bold type. (a) Alignment of the sequences of the N-terminal segments of the Iα and Iβ isoforms of G-kinase. Residue numbering is based on the Iα isoform. (b) "Helical wheel" representation of the sequence of G-kinase$_{1-39}$ amide. Residues that are conserved between Iα and Iβ isoforms are boxed in bold type. Conservative changes (D for E; R for K) are boxed in normal type. The N- and C-terminal residues are indicated by arrows. (c) "Helical net" representation of the sequence of G-kinase$_{1-39}$ amide. Residues with charged groups on their side chains are indicated by (+) and (−). The conserved negatively charged, hydrophobic, and positive–hydrophobic stripes are boxed.

studies have been carried out to assess the stability of the α-helical structure over a range of pH and temperature and to find suitable conditions for an NMR study.

(*i*) *pH Studies.* In spectra recorded at 40 °C, little change was observed as the pH was varied between 10.1 and 3.3. The sizes of the minima at 209 and 222 nm and the maximum at 191 nm (characteristics of α-helical structure) remained unaltered (Figure 2). The α-helical character was seen to be lost, and the calculated fraction of helical structure decreased as the pH was lowered below 3.3 [Figure 2 (inset)], in a manner which closely resembles the titration of acidic groups.

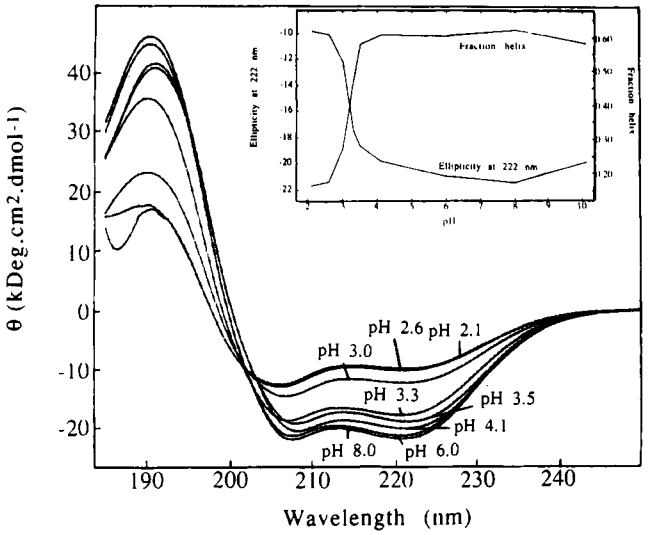

FIGURE 2: Circular dichroism spectra of G-kinase$_{1-39}$ amide recorded at 40 °C and a peptide concentration of 20 μM, at various pH values. Measured rotations are converted to mean residual ellipticities. For clarity, the spectrum recorded at pH 10.1 is omitted. (Inset) Variation of the mean residual ellipticity at 222 nm and of the calculated fraction of helical content with pH.

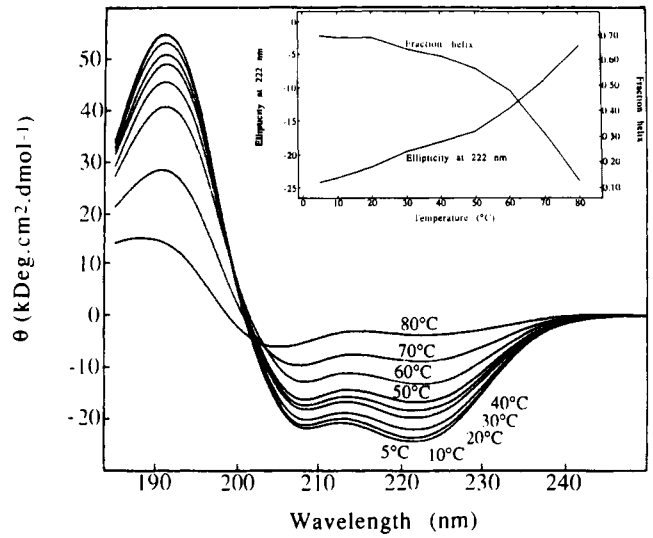

FIGURE 3: Circular dichroism spectra of G-kinase$_{1-39}$ amide recorded at pH 4.0 and a peptide concentration of 17 μM, with varying temperature. Measured rotations are converted to mean residual ellipticities. (Inset) Variation of the mean residual ellipticity at 222 nm and of the calculated fraction of helical content with temperature.

(*ii*) *Temperature Studies.* At pH 4.0 and a concentration of 17 μM, a gradual decrease in α-helical character was observed as the temperature was increased (Figure 3). The estimated percentage of α-helical structure was seen to decrease gently from 70% at 5 °C to 57% at 50 °C and then more rapidly above 60 °C [Figure 3 (inset)]. The stability of the structure, as determined by its sensitivity to temperature, was found to be a function of its concentration (Figure 4). Thus while spectra recorded at 2 μM showed a T_m of 67 °C, those at 20 μM gave a T_m of 75 °C, and at 200 μM the temperature could not be raised high enough to clearly define the T_m, which falls in the range 80–85 °C.

Isolated helices are, in principle, unstable and transient ("nascent") in aqueous solutions (Dyson et al., 1988; Saudek et al., 1991) and require the additional stabilization provided by tertiary structure or a less polar solvent (e.g., 1,1,1-trifluoroethanol). Thus the stability alone of the helical structure of G-kinase$_{1-39}$ amide may indicate that it is present as a dimer

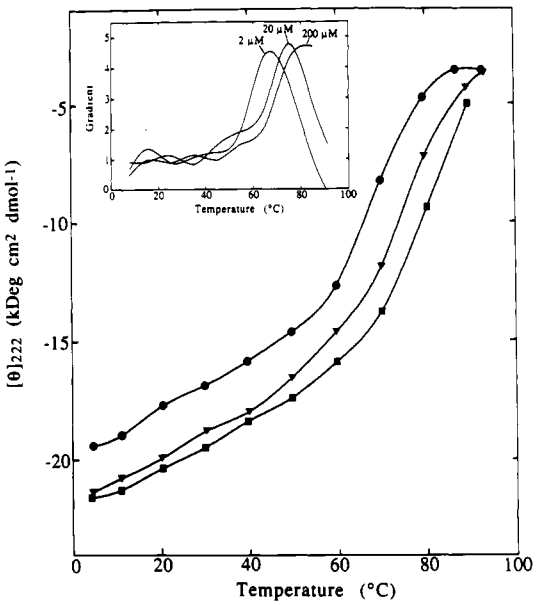

FIGURE 4: Mean residual ellipticity at 222 nm measured from CD spectra recorded at pH 4.0, between 4 and 94 °C. Data are shown for solutions of G-kinase$_{1-39}$ amide at concentrations of (●) 2 μM, (▼) 20 μM, and (■) 200 μM. (Inset) First derivatives of the temperature dependence curves.

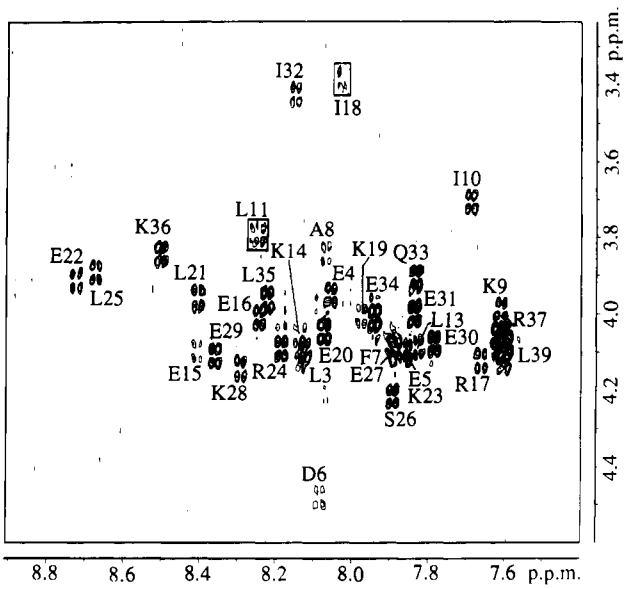

FIGURE 5: The "fingerprint region" of the COSY spectrum of G-kinase$_{1-39}$ amide recorded in ^1H_2O at pH 4.0 and 50 °C. Assignments are indicated by the single-letter codes and sequence numbers of the residues.

(or higher oligomer) in solution. This is confirmed by the concentration dependence of the T_m, which indicates that the peptide self-associates [see De Francesco et al. (1991)].

The behavior of the peptide with variation of pH can be understood if electrostatic interactions, which are necessary for the stabilization of either the dimeric association or the monomeric structure, are removed as glutamate side chains become protonated at low pH. Inspection of Figure 1b,c suggests that Glu 15, Glu 22, and Glu 29 may be key residues in this respect since they are likely to be involved in electrostatic interactions with lysine and arginine side chains on the opposite monomer.

Molecular Weight Determination by Ultracentrifugation. Measurement of the sedimentation coefficient and diffusion coefficient allows an estimate of the molecular weight of a species in solution to be calculated (Schachman, 1957; Chervenka, 1969) and hence an assessment of the degree of oligomerization to be made. The results for G-kinase$_{1-39}$ amide are as follows: the sedimentation coefficient, s, was calculated to be 1.88×10^{-13} s; the diffusion coefficient, D, was found to be 1.48×10^{-6} cm^2 s^{-1}. The molecular weight was thus calculated to be approximately 12800, with an estimated error of 10%. This value is 2.6 times the molecular weight of the monomer (4831.4) and so provides further evidence of the dimeric nature of the peptide in solution. That this value is greater than twice the molecular weight of the monomer might indicate the presence of higher oligomers in solution but may also be attributed in part to water molecules associated with the molecular species and to the lower precision of the method compared to the more rigorous sedimentation equilibrium method. (The full sedimentation equilibrium experiment was not performed due to the excessive run times required.)

Nuclear Magnetic Resonance Studies. The stability of the peptide to variations of pH and temperature allowed considerable freedom of choice in the conditions under which NMR studies could be performed. To minimize the rate of exchange of labile protons with solvent (Wüthrich & Wagner, 1979), while remaining within the limits set by the CD results, a pH of 4.0 was chosen. However, resonances in spectra recorded at 27 and 37 °C were found to be broad, and so the temperature was raised to 50 °C. While CD studies indicate that at lower concentrations some α-helical content is lost at such a temperature, this effect is likely to be negligible at the millimolar concentrations required for NMR studies.

The sequence of the peptide is remarkable in that just five amino acid types account for 32 of the 39 residues in the peptide. There are 13 residues with negatively charged side chains (12 of which are glutamates), 10 with positive charges, and 11 with large hydrophobic side chains. There is one aromatic side chain. As a result, there was considerable overlap in some regions of the spectra. Only one C$^\alpha$H resonance was observed downfield of the ^1H_2O resonance, and the methyl groups of the leucine and isoleucine residues were poorly dispersed. Nonetheless, the NH resonances were well enough resolved to facilitate the assignment of much of the sequence, as described below.

(*i*) *Assignment.* A number of spin systems could be readily classified according to amino acid type by analysis of COSY and TOCSY spectra (Wüthrich, 1986). The fingerprint region of the COSY spectrum recorded in ^1H_2O is shown in Figure 5. An AMX spin system was assigned to Phe 7 on the basis of NOEs to the only aromatic resonances in the spectrum. The lone downfield C$^\alpha$H resonance at 4.47 ppm has degenerate C$^\beta$H$_2$ resonances at 2.66 ppm and was assigned to Asp 6. A single spin system with connectivities characteristic of alanine residues was assigned to Ala 8. The spin systems of the three most upfield shifted C$^\alpha$H resonances were found to be those of the three isoleucine residues.

Two portions of the NOESY spectrum recorded in ^1H_2O are shown in Figure 6: these show NOEs between NH resonances and NOEs between NH resonances and the C$^\delta$H$_3$ resonances of leucine and isoleucine residues. A large number of strong NH–NH NOEs were observed, but due to severe overlap of C$^\alpha$H resonances in the range 4.0–4.2 ppm, C$^\alpha$H–NH NOEs were less easily resolved. However, an analysis of the two regions together allowed a large number of the backbone resonances to be assigned as shown. This was achieved by using the small number of residues identified above as markers and following NH–NH$_{i+1}$ connectivities. These were corroborated by the observation of some NH–NH$_{i+2}$ NOEs and both sequential C$^\alpha$H–NH$_{i+1}$ NOEs and longer range C$^\alpha$H–NH$_{i+3}$ and C$^\alpha$H–NH$_{i+4}$ NOEs from the better

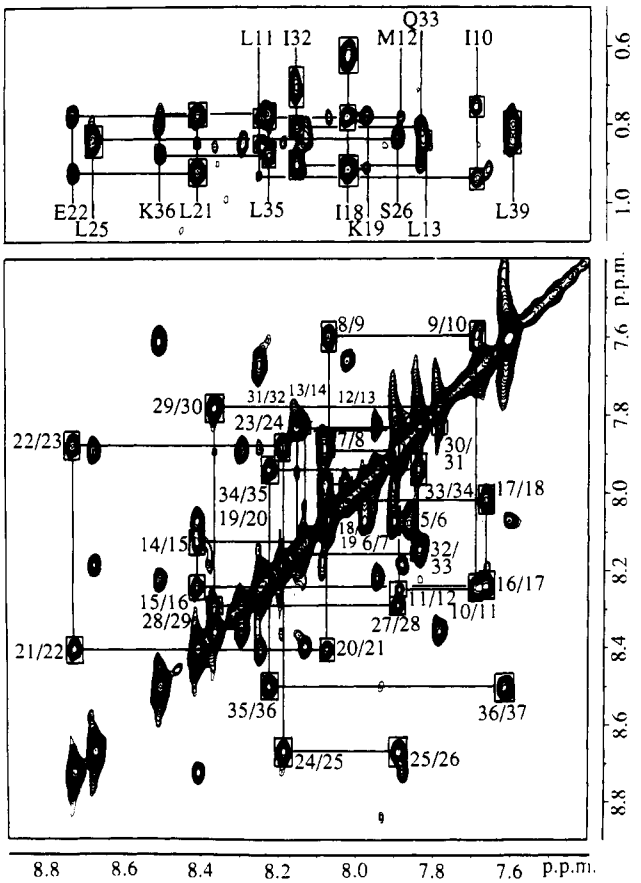

FIGURE 6: Portions of the NOESY spectrum of G-kinase$_{1-39}$ amide recorded in ^1H_2O at pH 4.0 and 50 °C with a mixing time of 200 ms. The lower section shows NOE connectivities between the NH resonances of neighboring amino acids. Cross-peaks are labeled with the pairs of sequence numbers of the corresponding residues. The upper section shows NOE connectivities between NH resonances and the $C^\beta H_3$ resonances of leucine and isoleucine side chains. Intraresidual NOEs are indicated by boxes with solid lines, indicating connectivities to the NH resonances of neighboring residues. NH resonances are labeled with the single-letter code and sequence number of the amino acid.

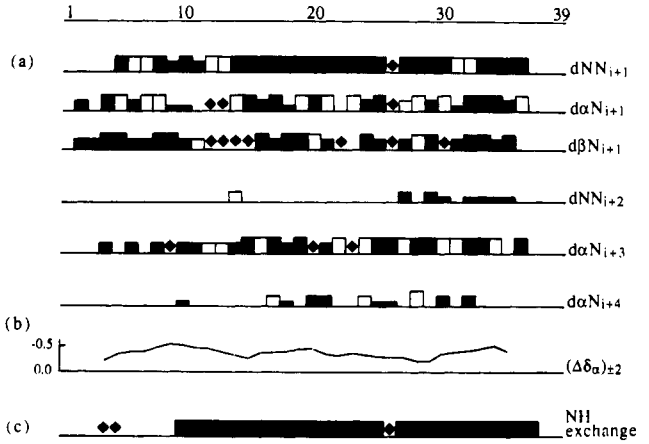

FIGURE 7: (a) Distribution and intensity of observed sequential and other interresidual NOEs. The notation is as described in footnote 1. The intensity of the NOE is indicated by the height of the bar. Unshaded bars indicate cases where overlap prevents clear assessment of the intensity. (♦) denotes cases where NOEs cannot be observed due to severe overlap or where the cross-peak is located too close to the diagonal. (b) Deviation of the chemical shifts of the $C^\alpha H$ resonances from "random coil" values, shown after smoothing by using a window of ±2 residues (Pastore & Saudek, 1991). (c) Residues with NH resonances which exchange slowly into ^2H_2O, indicated by shaded bars. (♦) denotes cases where assessment of NH exchange could not be made.

resolved $C^\alpha H$ resonances. For each backbone assignment, the spin system was then traced, by further analysis of COSY, TOCSY, and NOESY spectra, and determined to be consistent with the sequence.

In this manner, the assignment of the NMR spectrum of the peptide was achieved (Table I). The assignment is almost complete with only some side-chain resonances missing (e.g., not all seven lysine side chains could be fully assigned). All resonances of the leucine and isoleucine residues have been assigned, despite the overlap in the region of the spectrum containing their methyl resonances (0.7–1.0 ppm). The three arginine side chains have been fully assigned, including the $N^\epsilon H$ protons. The $N^\eta H_2$ resonances of Gln 33 have been assigned as have the resonances of the C-terminal amide group. At present, only residues Ser 1 and Lys 38 remain unassigned.

(*ii*) *Secondary Structure.* The pattern and the intensities of sequential and medium-range NOEs (i, $i + j$, where $j \leq 4$) are shown in Figure 7a. No long-range NOEs were observed. The pattern of NOEs expected for elements of secondary structure have been described (Wüthrich, 1986), and the pattern for α-helical structure (Saudek et al., 1989) is clearly in evidence here. Not all the possible NOEs for such a structure could be observed, often due to overlap, particularly of the $C^\alpha H$ resonances. (A ♦ symbol is used in Figure 7 where intensity is observed at the expected point in the NOESY spectrum but cannot be assigned unambiguously to a particular NOE.)

The pattern of NOEs indicates unbroken α-helical structure of the peptide between residues Glu 5 and Lys 36. Analysis of the assigned chemical shifts (Table I and Figure 7b) further supports this conclusion. Pastore and Saudek (1990) have described methods for analyzing the relationship between chemical shift and secondary structure. Application of the described methods to the $C^\alpha H$ assignments presented here, using a smoothing window of ±2 residues, shows upfield shifts throughout the assigned sequence, characteristic of helical structure.

(*iii*) *NH Exchange.* A large number of NH protons were seen to exchange slowly into ^2H_2O (Figure 7c). The slow exchange of labile protons indicates that the protons are relatively inaccessible to solvent and/or are involved in hydrogen bonding. Although the hydrogen-bonding partners cannot be detected by NMR, the pattern of slowly exchanging NH resonances for G-kinase$_{1-39}$ amide is expected for a stable α-helical structure. The NH protons of the residues at the N-terminal end of the helical structure (residues 6–9) were seen to exchange more rapidly into ^2H_2O than those of the remainder of the structure.

Distance Geometry Calculations. The calculated structures of the G-kinase$_{1-39}$ amide monomer are shown in Figures 8 and 9. The 10 best structures calculated from random initial conformations were fitted together over the backbone atoms of residues 11–37 to give an average pairwise rmsd value of 0.061 nm. Independent fitting of the backbone atoms of residues 4–11 gave an average pairwise rmsd value of 0.072 nm.

The structure is seen to be helical throughout almost the entire length of the peptide. While the N-terminal 11 residues appear ill-defined when residues 11–37 are overlaid (Figure 8), the backbone is found to adopt a helical conformation, whose orientation with respect to the following sequence is ill-defined. A kink in the helix is observed around Ser 26, and this is reproduced in structures calculated from initial structures with regular helical conformations. Figure 9 shows the proposed dimerization interface containing hydrophobic leucine

FIGURE 8: Stereoview of 10 calculated structures, overlaid by using the backbone atoms of residues 11–37. Five structures are taken from calculations with random initial conformations and five from calculations with helical initial conformations. Side-chain atoms are shown only for the residues of the leucine/isoleucine zipper.

and isoleucine residues and the charged glutamate and lysine side chains.

Conclusions

In this paper, G-kinase$_{1-39}$ amide has been shown to adopt an α-helical conformation which has been characterized by CD and NMR and which is stable over a wide range of pH values and temperature. The stability of the conformation is interpreted as an indication that the peptide exists as a dimer (or higher oligomer) of helical monomers. This has been confirmed both by the concentration dependence of the conformation to temperature and by the molecular weight measurement of the species in solution. The detection of only one set of resonances in the NMR spectrum and the absence of long-range NOEs indicate that the dimer is formed by a head-to-head (i.e., parallel), symmetrical arrangement of monomers. The formation of the dimer may now be modeled by using the monomer structures determined here by distance geometry methods.

The stability of the dimeric, α-helical conformation in solution can be rationalized in terms of the primary sequence of the peptide. The interaction of hydrophobic leucine and isoleucine side chains may be complemented by the interaction of glutamate side chains on one monomer with the lysine side chains on the other monomer. The dissociation of the dimer then requires elevated temperature or protonation of the glutamate side chains. In the Iβ isoform of G-kinase, this pattern is conserved with the two lysine residues being replaced by arginines and two of the three glutamates being replaced by aspartates. Furthermore, the sequence contains a concentration of negatively charged side chains at the N-terminus (SELEED-) and positively charged side chains at the C-terminus (-ELKRKL), which may serve to help balance the dipole of the helix. A sixth conserved hydrophobic residue is found at position 46 in the sequence of G-kinase and might be supposed to extend the leucine/isoleucine zipper further, although Chou–Fasman analysis does not support this suggestion (Landgraf et al., 1990). In addition, the cysteine residue at position 42 is able (under some conditions) to cross-link two monomers (Monken & Gill, 1980). This would not be possible if the helical structure were extended since the cysteine side chains would be located on opposite sides of the hydrophobic interface. Studies of longer peptides corresponding to the N-terminal sequence of the Iα isoform of G-kinase are in progress.

The leucine zipper domains of DNA transcriptional activators are found to be less stable than the leucine/isoleucine zipper domain of G-kinase, as measured by CD (O'Shea et al., 1989a,b; Saudek et al., 1991). A comparison of the sequences shows that of these, only the Fos protein contains negative and positive–hydrophobic stripes flanking the hydrophobic stripe of leucine side chains (although these are reversed with respect to G-kinase$_{1-39}$ amide). Despite this similarity, the Fos protein is exceptional among this set in that it does *not* readily form homodimers.

While the dimerization domain of G-kinase uses the same structural motif as the DNA transcriptional activators to achieve dimerization, it differs in a number of ways: the hydrophobic interface is not composed solely of leucine side chains but of alternating leucine and isoleucine side chains; the interaction is markedly stronger than that observed for the DNA transcriptional activators; and the motif is employed to dimerize an enzyme, in order to regulate its activity, rather than to position domains to enable binding.

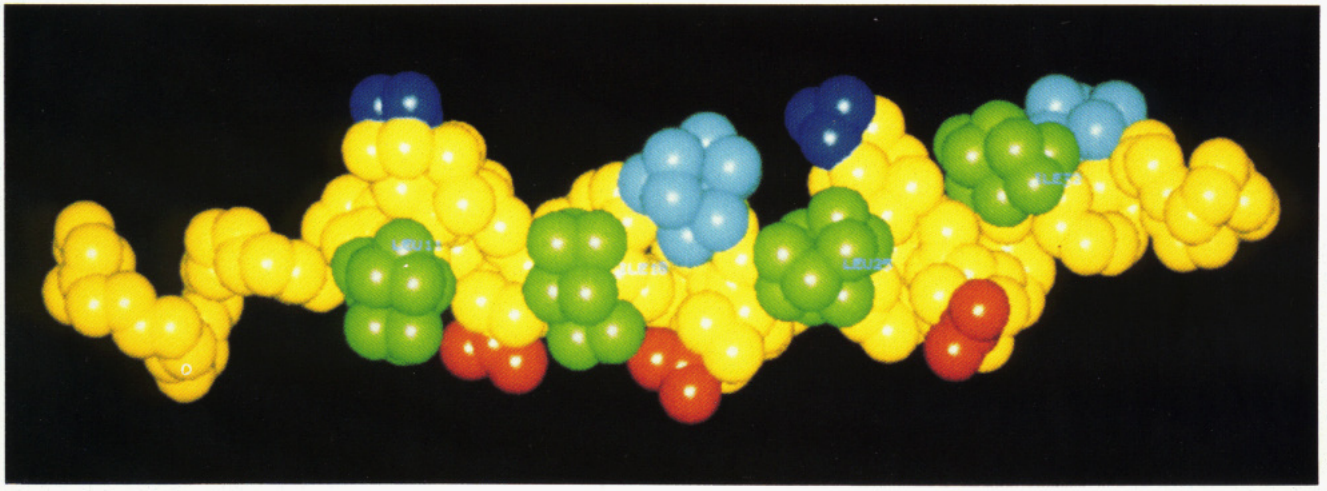

FIGURE 9: Space-filling representation of one calculated structure of the G-kinase$_{1-39}$ amide monomer. The backbone is shown together with the side chains of the leucine/isoleucine zipper (green), the stripe of glutamates (red), and the conserved positive–hydrophobic stripe created by lysine (blue) and leucine (light blue) side chains.

Table I: Assignment of the Resonances of G-Kinase$_{1-39}$ Amide

residue	chemical shifts (ppm)					
	HN	Hα	Hβ	Hγ	Hδ	Hε
Ser 1						
Glu 2		4.29	2.03, 1.95	2.32		
Leu 3	8.12	4.09	1.56, 1.48	1.48	0.82, 0.80	
Glu 4	8.05	3.95	2.01	2.32		
Glu 5	7.87	4.10	1.95	2.30		
Asp 6	8.08	4.47	2.66, 2.75			
Phe 7	7.90	4.07	2.78, 2.61		6.77	7.11
Ala 8	8.07	3.83	1.42			
Lys 9	7.61	3.98	1.94, 1.87	1.45	1.63	2.93
Ile 10	7.69	3.70	1.92	1.63, 1.13, 0.93	0.75	
Leu 11	8.25	3.79	1.54, 1.49	1.70	0.85, 0.78	
Met 12	7.89	4.01	2.27, 2.15	2.55		2.03
Leu 13	7.82	4.08	1.62, 1.57	1.79	0.84, 0.82	
Lys 14	8.12	4.05	2.10	1.71, 1.59	1.42	2.85, 2.71
Glu 15	8.40	4.09	2.18, 2.09	2.35		
Glu 16	8.24	4.00	2.20, 2.12	2.53, 2.43		
Arg 17	7.66	4.12	2.08, 2.00	1.77, 1.63	3.30, 3.12	7.01
Ile 18	8.02	3.38	1.95	1.87, 0.62, 0.78	0.91	
Lys 19	7.98	4.00	1.91, 1.87	1.44, 1.26	1.64, 1.58	2.92
Glu 20	8.07	4.04	2.22, 2.16			
Leu 21	8.40	3.95	2.11, 1.21	1.84	0.91, 0.78	
Glu 22	8.72	3.91	2.23, 1.98	2.66, 2.24		
Lys 23	7.87	4.10	1.99, 1.93	1.52		
Arg 24	8.18	4.09	1.99, 1.86	1.84, 1.67	3.15	7.44
Leu 25	8.67	3.89	1.78, 1.67	1.60	0.84, 0.82	
Ser 26	7.89	4.21	4.01			
Glu 27	7.89	4.10	2.31, 2.27	2.15		
Lys 28	8.29	4.13	2.08	1.63	1.46	2.92, 2.80
Glu 29	8.36	4.10	2.17, 2.08	2.41, 2.32		
Glu 30	7.78	4.07	2.19	2.50, 2.44		
Glu 31	7.83	4.00	2.23, 2.14	2.53, 2.51		
Ile 32	8.15	3.42	1.93	1.81, 0.70, 0.80	0.90	
Gln 33	7.83	3.90	2.16, 2.11	2.49, 2.42		7.28, 6.70
Glu 34	7.94	4.01	2.18, 2.09	2.50, 2.35		
Leu 35	8.22	3.95	1.97, 1.24	1.87	0.87, 0.76	
Lys 36	8.50	3.83	1.82, 1.80	1.29	1.57	2.87, 2.81
Arg 37	7.62	4.03	1.91	1.79, 1.62	3.18	7.16
Lys 38						
Leu 39	7.59	4.09	1.67, 1.57	1.64	0.83, 0.80	
CT NH_2	6.98, 6.91					

This paper is the first report of the experimental determination of the structure of any domain within G-kinase. It seems unlikely that the N-terminal domain of the native enzyme is conformationally different in solution, because of the remarkable stability of its helical structure described in this paper. The demonstration that the N-terminal domain of G-kinase dimerizes in the absence of a disulfide bond at Cys 42 suggests that this bond is probably not important in maintaining the quaternary structure of the enzyme. It is possible that mild denaturation of G-kinase could unwind part of the dimerization domain and permit cross-linking to occur. This would explain the conflicting reports regarding the existence of the disulfide bridge (Monken & Gill, 1980; Takio et al., 1983).

To date, two isoforms of G-kinase have been purified, both of which are homodimeric (Lincoln et al., 1988; Wolfe et al., 1989). Given the similarities between the N-terminal domains of the two isoforms, it is possible that G-kinase heterodimers may also exist, or could be formed experimentally. Also, the close proximity of the final residue of the heptad repeat (Leu 46) and the autophosphorylation site at Thr 58 suggests that the N-terminal helix may be important in maintaining the conformation of the autoinhibitory sequence within the G-kinase enzyme. Experiments which have been performed to address the role of the N-terminus (Landgraf & Hofmann, 1989; Landgraf et al., 1990) have used a proteolytically modified enzyme which lacks both the autophosphorylation site and the dimerization domain. Hence the determination of the precise role of the leucine/isoleucine zipper in controlling the enzymic activity of G-kinase must await more detailed proteolytic or mutagenesis experiments.

ACKNOWLEDGMENTS

We thank Patrick Bortmann for his assistance in the preparation of the figures and Guy Daney De Marcillac of the IBMP, CNRS, Strasbourg, for determining the molecular weight of G-kinase$_{1-39}$ amide by ultracentrifugation.

REFERENCES

Aitken, A., Hemmings, B. A., & Hofmann, F. (1984) *Biochim. Biophys. Acta 790*, 219–225.

Anil-Kumar, Ernst, R. R., & Wüthrich, K. (1980) *Biochem. Biophys. Res. Commun. 95*, 1–6.

Aue, W. P., Bartholdi, E., & Ernst, R. R. (1976) *J. Chem. Phys. 64*, 2229–2246.

Bax, A., & Davis, D. G. (1985) *J. Magn. Reson. 65*, 355–366.

Braun, W., & Go, N. (1985) *J. Mol. Biol. 186*, 611–626.

Braunschweiler, L., & Ernst, R. R. (1983) *J. Magn. Reson. 53*, 521–528.

Brendel, V., & Karlin, S. (1989) *Nature 341*, 574–575.

Chang, C. T., Wu, C.-S. C., & Yang, J. T. (1978) *Anal. Biochem. 91*, 13–31.

Chervenka, C. H. (1969) *A manual of methods for the analytical ultracentrifuge*, Beckman Instruments Inc., Palo Alto, CA.

Chou, P. Y., & Fasman, G. D. (1977) *J. Mol. Biol. 115*, 135–175.

Cohn, E. J., & Edsall, J. T. (1943) in *Proteins, Amino Acids and Peptides*, pp 370–381, Hafner Publishing Co., New York.
De Francesco, R., Pastore, A., Vecchio, G., & Cortese, R. (1991) *Biochemistry 30*, 143–147.
Dyson, H. J., Rance, M., Houghten, R. A., Wright, P. E., & Lerner, R. A. (1988) *J. Mol. Biol. 201*, 201–217.
Ecker, T., Göbel, C., Hullin, R., Rettig, R., Seitz, G., & Hofmann, F. (1989) *Circ. Res. 65*, 1361–1369.
Edelman, A. M., Blumenthal, D. K., & Krebs, E. G. (1987) *Annu. Rev. Biochem. 56*, 567–613.
Fiscus, R. R., Rapoport, R. M., & Murad, F. (1984) *J. Cyclic Nucleotide Protein Phosphorylation Res. 9*, 415–425.
Flockerzi, V., Speichermann, N., & Hofmann, F. (1978) *J. Biol. Chem. 253*, 3395–3399.
Gill, G. N., Holdy, K. E., Walton, G. M., & Kanstein, C. B. (1976) *Proc. Natl. Acad. Sci. U.S.A. 73*, 3918–3922.
Gill, G. N., Walton, G. M., & Sperry, P. J. (1977) *J. Biol. Chem. 252*, 6443–6449.
Heil, W. G., Landgraf, W., & Hofmann, F. (1987) *Eur. J. Biochem. 168*, 117–121.
Hofmann, F., & Sold, G. (1972) *Biochem. Biophys. Res. Commun. 49*, 1100–1107.
Hofmann, F., Gensheimer, H.-P., & Göbel, C. (1985) *Eur. J. Biochem. 147*, 361–365.
Hoult, D. I., & Richards, R. E. (1975) *Proc. R. Soc. London, A 344*, 311–320.
Jeener, J., Meier, B. H., Bachmann, P., & Ernst, R. R. (1979) *J. Chem. Phys. 71*, 4546–4553.
Kouzarides, T., & Ziff, E. (1989) *Nature 340*, 568–571.
Kuo, J. F. (1974) *Proc. Natl. Acad. Sci. U.S.A. 71*, 4037–4041.
Landgraf, W., & Hofmann, F. (1989) *Eur. J. Biochem. 181*, 643–650.
Landgraf, W., Hullin, R., Göbel, C., & Hofmann, F. (1986) *Eur. J. Biochem. 154*, 113–117.
Landgraf, W., Hofmann, F., Pelton, J. T., & Huggins, J. P. (1990) *Biochemistry 29*, 9921–9928.
Landschulz, W. H., Johnson, P. F., & McKnight, S. L. (1988) *Science 240*, 1759–1764.
Lincoln, T. M., Dills, W. L., Jr., & Corbin, J. D. (1977) *J. Biol. Chem. 252*, 4269–4275.
Lincoln, T. M., Flockhart, D. A., & Corbin, J. D. (1978) *J. Biol. Chem. 253*, 6002–6009.
Lincoln, T. M., Thompson, M., & Cornwell, T. L. (1988) *J. Biol. Chem. 263*, 17632–17637.
Lohmann, S. M., Walter, U., Miller, P. E., Greengard, P., & De Camilli, P. (1981) *Proc. Natl. Acad. Sci. U.S.A. 78*, 653–657.
Macura, S., Huang, Y., Suter, D., & Ernst, R. R. (1981) *J. Magn. Reson. 43*, 259–281.
Marion, D., & Wüthrich, K. (1983) *Biochem. Biophys. Res. Commun. 113*, 967–974.
Monken, C. E., & Gill, G. N. (1980) *J. Biol. Chem. 255*, 7067–7070.
O'Shea, E. K., Rutkowski, R., & Kim, P. S. (1989a) *Science 243*, 538–542.
O'Shea, E. K., Rutkowski, R., Stafford, W. F., III, & Kim, P. S. (1989b) *Science 245*, 646–648.
Pastore, A., & Saudek, V. (1990) *J. Magn. Reson. 90*, 165–176.
Rance, M. (1987) *J. Magn. Reson. 74*, 557–564.
Sandberg, M., Natarajan, V., Ronander, I., Kalderon, D., Walter, U., Lohmann, S. M., & Jahnsen, T. (1989) *FEBS Lett. 255*, 321–329.
Saudek, V., Atkinson, R. A., Williams, R. J. P., & Ramponi, G. (1989) *J. Mol. Biol. 205*, 229–239.
Saudek, V., Pastore, A., Castiglione Morelli, M. A., Rainer, F., Gausepohl, H., Gibson, T., Weih, F., & Rösch, P. (1990) *Protein Eng. 4*, 3–10.
Saudek, V., Pasley, H. S., Gibson, T., Gausepohl, H., Frank, R., & Pastore, A. (1991) *Biochemistry* (in press).
Schachman, H. K. (1957) *Methods Enzymol. 4*, 32–103.
Soderling, T. R. (1990) *J. Biol. Chem. 265*, 1823–1826.
Takio, K., Smith, S. B., Walsh, K. A., Krebs, E. G., & Titani, K. (1983) *J. Biol. Chem. 258*, 5531–5536.
Takio, K., Wade, R. D., Smith, S. B., Krebs, E. G., Walsh, K. A., & Titani, K. (1984) *Biochemistry 23*, 4207–4218.
Wernet, W., Flockerzi, V., & Hofmann, F. (1989) *FEBS Lett. 251*, 191–196.
White, M. K., & Weber, M. J. (1989) *Nature 340*, 103–104.
Wolfe, L., Corbin, J. D., & Francis, S. H. (1989) *J. Biol. Chem. 264*, 7734–7741.
Wüthrich, K. (1986) *NMR of Proteins and Nucleic Acids*, J. Wiley & Sons, New York.
Wüthrich, K., & Wagner, G. (1979) *J. Mol. Biol. 130*, 1–18.
Wüthrich, K., Billeter, M., & Braun, W. (1983) *J. Mol. Biol. 169*, 949–961.